RSC Advances

PAPER

View Article Online
View Journal | View Issue

Cite this: *RSC Adv.*, 2025, **15**, 12987

Enzyme-immobilized graphene oxide-based electrochemical biosensor for glutathione detection

Neeta Ukirade,[ab] Upasana Choudhari,[c] Sunil Bhapkar,[d] Umesh Jadhav,[d] Shweta Jagtap *[c] and Sunit Rane *[a]

Glutathione acts as a natural antioxidant in the human body and the reduction of its content is a sign of oxidative stress. In this study, a sensitive electrochemical sensor was developed using laccase enzyme immobilized onto graphene oxide (GO) for detection of glutathione. The surface of the indium tin oxide (ITO) was modified with GO *via* a drop casting method. Subsequently, laccase was immobilized onto the modified ITO decorated with GO. The modified electrode was characterized using field-emission scanning electron microscopy (FESEM), X-ray photoelectron spectroscopy (XPS), Fourier transform infrared spectroscopy (FTIR), cyclic voltammetry (CV) and electrochemical impedance spectroscopy (EIS). The FTIR spectra of laccase/GO confirmed the successful immobilization of laccase onto GO sheets. FESEM analysis revealed the transformation from a layered, wrinkled structure to a compact, smooth surface with spherical laccase, confirming successful enzyme integration. Raman analysis confirmed successful laccase immobilization onto GO, as evidenced by structural changes in the D and G bands, highlighting the modification of the material. The cyclic voltammetry measurements revealed that laccase/GO/ITO exhibited better electrocatalytic activity toward oxidation of GSH in acetate buffer solution than the bare ITO electrode. This newly developed electrode exhibited a good response to glutathione with a wide linear range from 1 μM to 100 μM, a limit of detection of 0.89 μM and high sensitivity (6.51 μA μM^{-1}). Furthermore, it exhibited excellent selectivity, repeatability, and long-term stability. The modified electrode was successfully used for the detection of GSH in a real sample, offering satisfactory results.

Received 27th December 2024
Accepted 1st April 2025

DOI: 10.1039/d4ra09033k

rsc.li/rsc-advances

Introduction

Development of biosensors is receiving a lot of attention in the biomedical and healthcare fields owing to its extensive use in medicine, clinical care and food processing. A biosensor is an analytical device that measures the changes in biological elements or materials, such as cells, tissues, enzymes, and microorganisms, and converts them into electrical signals. The output of the transducer will either be current or voltage, depending on the kind of enzyme and components utilized in the biological element.[1–3] Biosensors are made up of various elements, including an analyser, bio receptor, transducer, electronics, and a reader display. Novel nanobiosensors can be developed by combining biological sensing components with organic, inorganic or hybrid nanomaterials to detect chemical or biological substances. Rapid advances in nanotechnology have led to the development of innovative nanomaterials and nanodevices that hold promise for use in biomedical and healthcare applications in the future.[4–8] The first biosensor was created in 1916 when proteins were immobilized on activated charcoal. Later, Clark furthered the technology for the amperometric detection of glucose.[9] The advancement of nanomaterial-based biosensors opens a new way for the identification and real-time monitoring of biomarkers linked to a variety of diseases and their treatments. Electrochemical biosensors based on nanomaterials have changed the outlook for traditional biosensors by enhancing their performance in terms of sensitivity, stability, and selectivity for the detection of different biomolecules.[10–12] Nanomaterials with special chemical and physical properties are advantageous for developing efficient biosensors owing to the high surface area for loading enzymes. Carbon-based nanomaterials, particularly graphene, have contributed to improved insights in the fields of bioengineering and medicine.[13,14] In comparison with other materials, graphene is recognised as the lightest material, and it is used in practically every aspect of life owing to its exceptional qualities, including its high surface area, excellent electrical conductivity,

[a]*Centre for Materials for Electronics Technology (C-MET), Panchawati, Off. Dr Bhabha Road, Pune-411008, India. E-mail: sunitrane@yahoo.com*

[b]*Pratibha College of Commerce and Computer Studies, Pune, India*

[c]*Department of Electronic and Instrumentation Science, Savitribai Phule Pune University, Pune-411007, India. E-mail: shweta.jagtap@gmail.com*

[d]*Department of Microbiology, Savitribai Phule Pune University, Pune-411007, India*

extensive strength, simplicity of functionalization, superior thermal conductivity, chemical inertness, and gas impermeability.[15–17] Graphene oxide (GO) has a significantly better capability for protein adsorption compared with other carbonaceous materials with a wide surface area. Its physicochemical characteristics and structure are said to be advantageous for alterations in enzyme activity. Enzymatic electrochemical biosensors have gained significant interest in recent times owing to their efficaciousness and stability.[18,19] The human body is made up of several biomolecules that control physiological processes, including proteins, carbohydrates, nucleic acids, and amino acids. Abnormal concentrations of these biomolecules cause a number of diseases. As a result, selective and sensitive detection of these biomolecules is crucial for pharmacological compositions and clinical diagnostics.[20,21] Glutathione (GSH) is a tripeptide of L-glutamyl-L-cysteinyl-glycine thiol molecule with a low intracellular molar mass and is an essential antioxidant cofactor for the metabolism of living cells. Glutathione concentration changes to low levels are connected to diseases such as leukaemia, pre-mature arteriosclerosis, diabetes, Alzheimer's, and AIDS-related dementia. As a result, there has been a growing interest in and demand for this biomarker's accurate detection during the past ten years.[22] The preservation of enzyme activity, involvement in bioreductive reactions, transport of amino acids, and detoxification of free radicals, hydrogen peroxide, and toxins are all significant functions of reduced glutathione (GSH).[23,24] Glutathione inhibits laccase, a frequently utilised multicopper oxidase for oxygen reduction.

In this research, the developed biosensor utilizes the catalytic activity of laccase combined with the unique properties of GO to achieve high sensitivity and selectivity. The interaction between the analyte (glutathione) and the enzyme leads to measurable changes in the solution's properties, which are then detected by the biosensor. We focused on laccase's potential application as a glutathione sensor.[25,26] In this study, we used an electrochemical biosensor based on laccase to examine the electrochemical behaviour of GSH. First, we synthesized GO which was deposited on the surface of bare indium tin oxide (ITO). Then, laccase was immobilized onto the electrode surface using a gelatin membrane, which was cross-linked by glutaraldehyde. Furthermore, the electrochemical behavior of the modified electrode was investigated by cyclic voltammetry. The results of this study indicate that GO may be used as a potential sensing material in conjunction with an enzyme to detect GSH. The modified electrode showed high selectivity for the determination of GSH in real samples.

Experimental

Materials

Glutathione (GSH), cysteine (CYS), dopamine (DA), ascorbic acid (AA), uric acid (UA), glutaraldehyde, and laccase were purchased from Sigma-Aldrich. Graphite powder, potassium permanganate, sulfuric acid (99.99%), hydrochloric acid, and sodium nitrate were purchased from Merck Company. All other compounds were analytical reagent grade and all solutions were made with deionized water. 0.1 M phosphate buffer solution (PBS, pH 7) was used as the background electrolyte. A stock solution of 1 mM GSH was prepared.

Preparation of laccase/GO/ITO electrode

An ITO-coated piece of glass slide (0.5 × 0.5 cm^2) was used as the substrate. Prior to usage, the substrate was cleaned using ultrasonic cleaning in deionized water and ethanol. GO was prepared using Hummer's method.[27–29] Furthermore, GO was electrodeposited on the surface of bare ITO by the drop casting method. The electrode was dried under an infrared (IR) lamp until the solvent evaporated and the electrode surface was fully dry. In the next step, laccase was immobilized onto GO/ITO. For this purpose, 20 mg of laccase was diluted in 100 μL of phosphate buffer solution (pH 7.0). Then, 25 U of laccase and 12 mg of gelatin were mixed at 38 °C in potassium phosphate buffer (pH 7.0, 100 μL). Next, 25 μL of the mixed solution was spread over the modified electrode surface and allowed to dry at 4 °C for 1 h. Finally, it was immersed in 2.5% glutaraldehyde in phosphate buffer (50 mM, pH 7.0) for 5 min for cross-linkage.[30] To evaluate the electrochemical behavior of the developed sensors, cyclic voltammetry was used with a three-electrode system with a working electrode of 0.25 cm^2 electrochemical active surface area.

Characterization

The crystallographic structure of the samples were studied using X-ray diffraction (XRD) analysis using a Bruker D8 Advance with a monochromator of CuKα radiation ($\lambda = 1.541\,87$ Å) over a 2θ range of 5–80°. The surface morphology and microstructural analysis of the samples were performed using a NOVA NanoSEM 450 (Thermo Fisher Scientific, USA). The instrument was operated at an accelerating voltage ranging from 1 to 30 kV, depending on the sample's conductivity. Elemental composition analysis was performed using an energy-dispersive X-ray spectroscopy (EDS) system (Bruker XFlash 6I30). Fourier transform infrared spectroscopy (FTIR) was performed using a Shimadzu FTIR-8900 to identify the chemical functional groups present in all synthesized materials, covering a spectral range of 4000–400 cm^{-1}. The K-Lyte potentiostat is used for conducting cyclic voltammetry (CV) experiments as part of electrochemical analyses. For the electrochemical measurements, a standard three-electrode cell assembly made up of an Ag/AgCl as reference electrode, a Pt counter electrode and an ITO working electrode.

Results and discussion

(A) Physical characterization of the nanocomposite

Fourier transforms infrared spectroscopy (FTIR). The functional groups involved in the interaction of nanocomposites are examined using Fourier transform infrared spectroscopy (FTIR) from 4000 to 500 cm^{-1} (Fig. 1). The peaks observed at 3177 cm^{-1}, 1619 cm^{-1}, and 1031 cm^{-1} correspond to the O–H stretching, O–H stretching, C=O stretching, and C–O stretching vibration, indicating that the graphene was oxidized and the

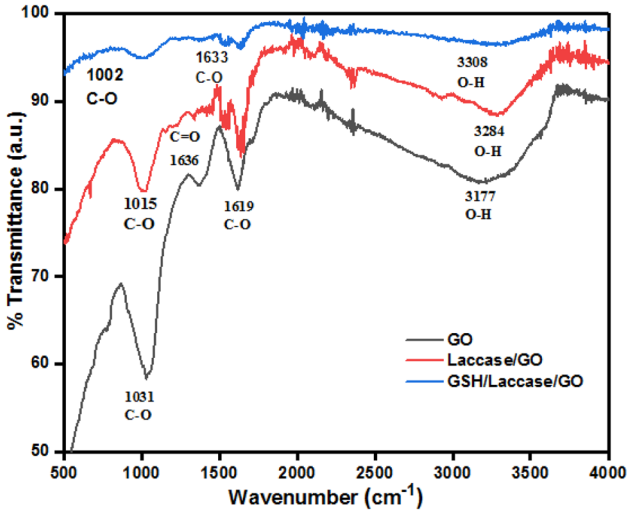

Fig. 1 FTIR spectra of GO, laccase/GO and GSH/laccase/GO.

GO product could be successfully dispersed in water.[31] For laccase, the peak at 3284 cm^{-1} was caused by O–H stretching in laccase. The spectrum also showed an amide I band at 1636 cm^{-1} due to C=O stretching and a band at 1165–948 cm^{-1} characteristic of laccase.[32] The FTIR spectrum of laccase/GO showed that laccase was successfully immobilized onto GO due to presence of characteristic peaks of laccase and the GO.

Morphological studies. Field emission scanning electron microscopy (FESEM) and energy dispersive spectroscopy (EDS) measurements were used to study the morphology and the elemental distribution of GO nanosheets and the laccase/GO surface. Fig. 2a–e represents the top view and cross-sectional view FESEM images of GO and laccase/GO. The GO sheets exhibit a flaky, layered structure (Fig. 2a), with the higher-magnification view highlighting the fine surface texture and smaller wrinkle shape morphology of GO sheets (Fig. 2b). The surface morphology significantly changes after the incorporation of laccase (Fig. 2c). The spherical laccases were uniformly distributed on the laccase/GO surface, indicating that the laccase was stably immobilized on GO. Zhou *et al.*[33] reported enzyme-enhanced adsorption of laccase-immobilized graphene oxide for micropollutant removal, where morphological analysis revealed that GO exhibits a flat layered structure with a smooth surface and crumpled edges. Additionally, spherical laccases were evenly distributed on the laccase/GO surface indicating stable immobilization of laccase on GO sheets. These structural observations are well aligned with our studies. In the cross-sectional view, GO and laccase/GO films appear compact, although the laccase/GO film exhibits slight interlayer and surface modifications (Fig. 2d and e). EDS images indicate the presence of carbon and oxygen functionalities on the surface of the GO sheets (Fig. 2f), while laccase/GO showed C, O, and N elements related to laccase, confirming the successful immobilization of laccase onto GO (Fig. 2g).

Raman spectroscopy analysis. Raman spectroscopy gives information about the phases and defects present in the material. Raman spectra of GO and laccase/GO is shown in

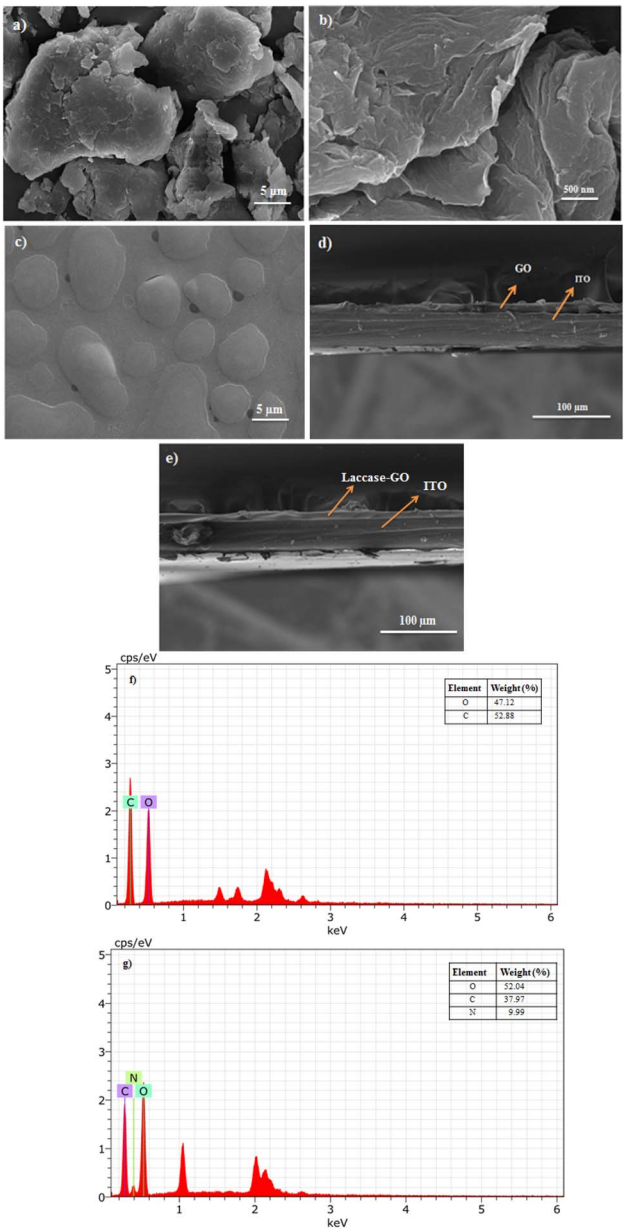

Fig. 2 FESEM surface image of (a) GO and (b) high magnification images of GO and (c) laccase/GO. Cross-sectional images of (d) GO and (e) laccase/GO. EDS spectra of (f) GO and (g) laccase/GO.

Fig. 3. The spectra show two characteristic peaks: a D-band at 1350 cm^{-1} associated with defects and disorder and a G-band at 1585 cm^{-1} associated with vibration of carbon atoms that are sp^2-bonded in a two-dimensional hexagonal lattice.[34,35] There are slight alterations in the Raman spectra for laccase/GO. The increase in the intensity of the D peak and widening of the G band correlates with the level of disorder. This structural disorder is due to the interaction of the enzyme with GO. The slight increase in I_D/I_G from 0.98 (GO) to 1.02 (laccase/GO) suggests that laccase treatment introduces slight structural disorder, verifying that the laccase immobilization onto GO was successful.

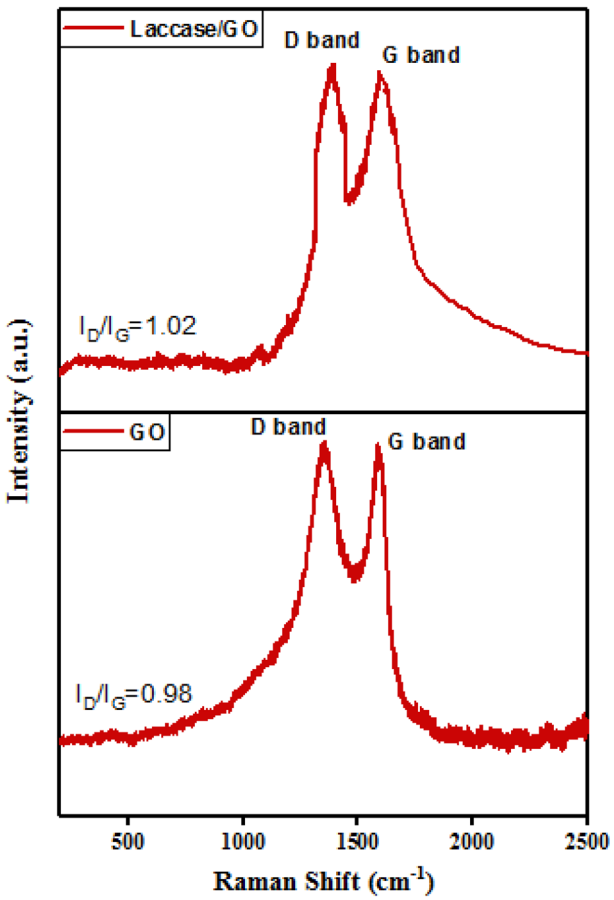

Fig. 3 Raman spectra of GO and laccase/GO.

X-ray diffraction (XRD). The structural properties of GO and laccase/GO films were studied using X-ray diffraction (XRD) analysis, which revealed the crystal structure of GO and laccase/GO films. The XRD patterns of GO and laccase/GO are shown in Fig. 4. The peak at $2\theta = 10.39°$ from GO powder corresponds to an interlayer distance of 0.81 nm calculated by the Bragg equation, which matches the reports available in the literature.[33] The presence of this peak indicates the oxidation of graphite and the formation of oxygen-containing functional groups. However, the peak at $2\theta = 16.5$ in laccase/GO could be attributed to the immobilization of laccase on the GO surface as reported by Zhou *et al.*[33]

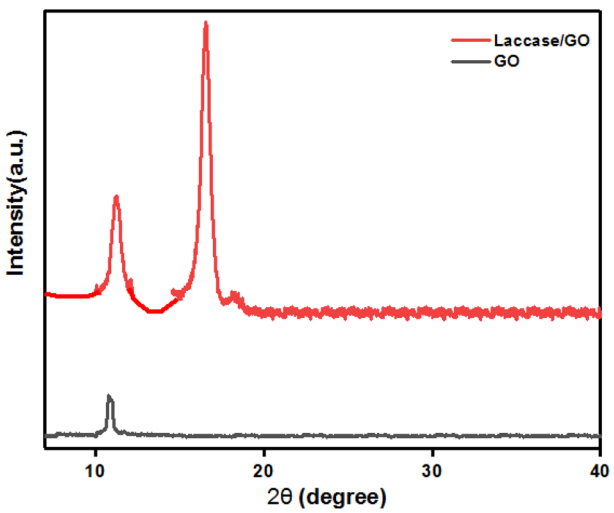

Fig. 4 X-ray diffraction patterns of GO and laccase/GO.

X-ray photoelectron spectroscopy (XPS). X-ray photoelectron spectroscopy (XPS) is one of the most popular methods for determining the chemical composition of material surfaces. It is an effective technique for researching surface reactions at vacuum levels, even at the monolayer level. Surface analysis using XPS has been applied in a number of industries, including mineral processing, corrosion, electronics, nanomaterials, biomedicine, automotive, and aerospace, among others. Additionally, XPS analysis can reveal information the composition, orientation of molecules adsorbed on the surface, structure of surface layers, and the distribution of elements on the surface.[36,37] Fig. 5a and d shows the survey scan spectrum of the GO and laccase/GO. For GO, the bands centered at 284.74 and 530.77 eV are associated with C 1s and O 1s, respectively. The C 1s XPS spectrum of GO indicates the degree of oxidation with three components which correspond to C atoms in different functional groups (Fig. 5b): the non-oxygenated ring C=C at 283.3 eV, C–C at 284.1, the C atom in the C–OH bond at 285.6 eV, C–O at 286 eV, and the carbonyl C (C=O) at 287.13 eV. Similarly, the oxygen 1s (O 1s) spectrum of GO showed two functional groups in the spectra: O–C=O at 530.5 eV and C=O at 531.2 eV, indicating that the graphene was oxidized (Fig. 5c). XPS spectra for C 1s core levels of laccase as deposited layers on GO contain peaks corresponding to C–C or C–H bonds at 283.4 eV, C–C bonds at 284.6 eV, C–O bonds at 285.8 eV, and C–O–C bonds at 286.5 eV (Fig. 5e). The peak areas indicate that the laccase layer deposited on GO is characterized by a higher content of C–C or C–H. Similarly, O 1s core levels of spectra showed three O components such as O–C=O at 530.7 eV, C=O at 531.5 eV (Fig. 5f). XPS spectra for the N 1s core levels of laccase as-deposited layers on GO show two peaks that come from amino groups: amide at 398.5 eV and imide at 400.06 eV (Fig. 5g), confirming the presence of laccase molecules.[38,39]

(B) Electrochemical behavior

The surface characteristics of the fabricated electrode surface at various stages of modification were examined using the CV technique in 5 mM $[Fe(CN)_6]^{3-/4-}$ solution at a scan rate of 40 mV s^{-1}. Fig. 6 shows the CVs of the bare ITO electrode and ITO modified with GO and GO/ITO modified with laccase. Well-defined redox peaks were observed for bare ITO. Due to GO, the redox peak currents increase after the ITO was modified with GO.[40] Laccase catalyses the single electron oxidation of various phenolic compounds. The performance of laccase-based electrochemical biosensors is improved by the introduction of graphene-based nanomaterial owing to its high conductivity, large specific surface area, flexibility and chemical inertness. Furthermore, the redox peak current increases by placing laccase on modified ITO.

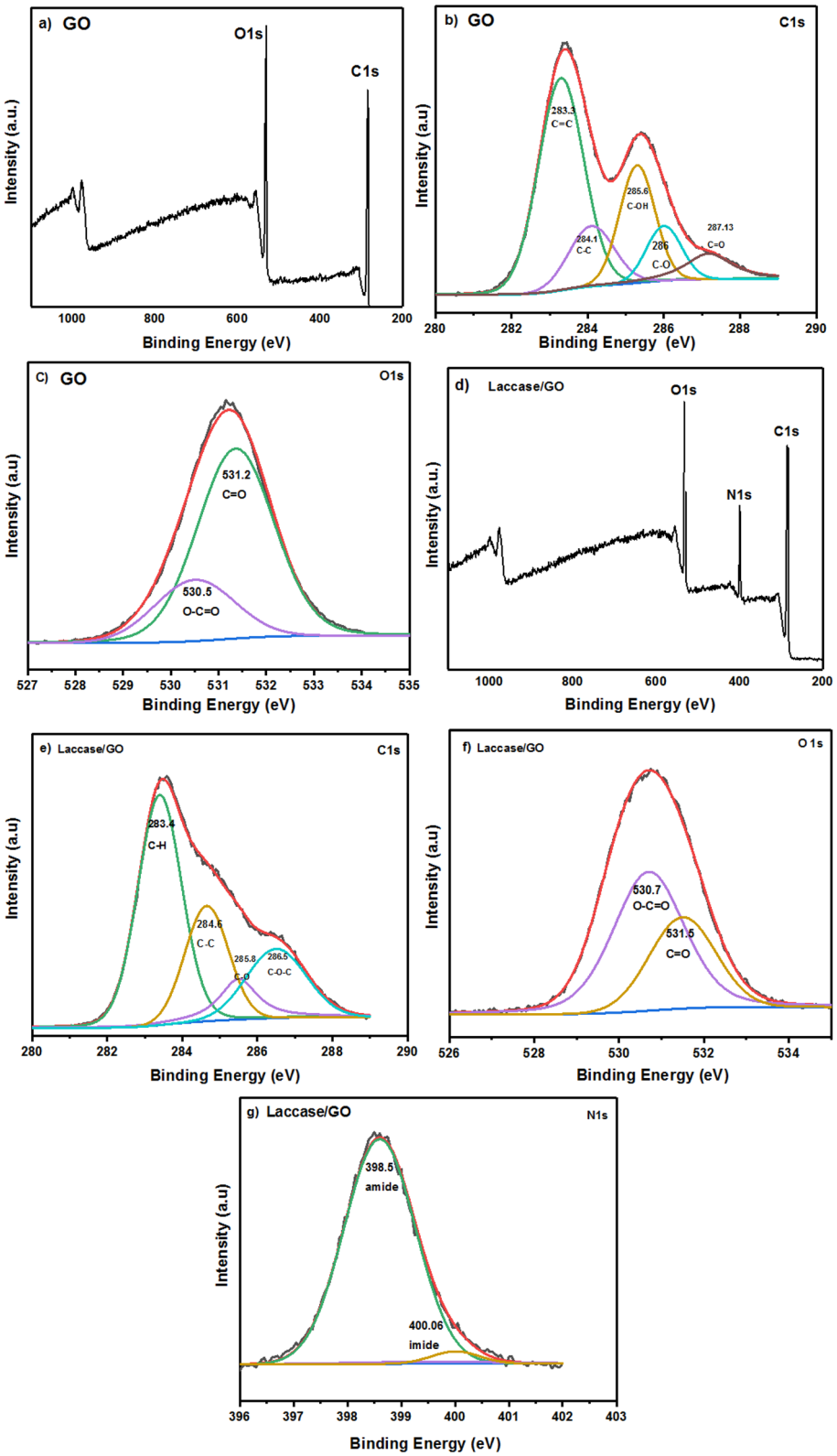

Fig. 5 XPS spectra of GO and laccase/GO. (a and d) Survey spectrum; (b and e) C 1s spectrum; (c and f) O 1s spectrum of GO and laccase/GO; (g) N 1s spectrum of laccase/GO.

Optimization of the experimental conditions

Effect of pH. It is generally recognised that the electrolyte's pH plays a significant role in electrochemical techniques. The electrocatalytic capabilities and pH of the modified electrode are inseparably connected. Electrode materials often exhibit stable behaviour near neutral pH, making it suitable for

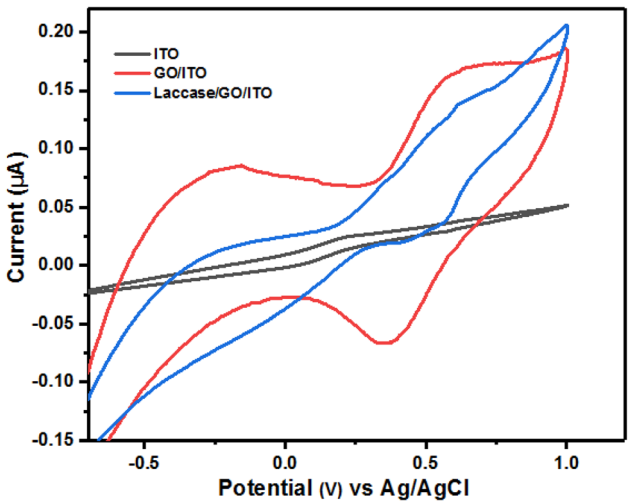

Fig. 6 Cyclic voltammograms of bare ITO, GO/ITO and laccase/GO/ITO in a 1.0 mM $[Fe(CN)_6]^{3-/4-}$ solution containing 0.1 M KCl.

studying fundamental electrochemical processes without interference from extreme pH conditions. Neutral pH (around pH 7) is relevant to many practical applications.[41] The pH value for the detection of glutathione plays a key role due to disulphide bond formation in the oxidation of glutathione. As a result, the electrochemical behaviour of the modified electrode for different pH values was investigated. The peak potential (E_p) shifts towards less positive values as the pH increases (Fig. 7a). This shift suggests that the oxidation process is influenced by proton concentration, which affects the redox potential. The shift in peak potential is indicative of proton-dependent reactions occurring at the electrode surface.[42,43] As the pH increased, glutathione's oxidation peak current first gradually increased, then gradually reduced. The highest value was obtained at pH 7. Therefore, pH 7 was selected as the ideal value for the following experiment.

Catalytic effect. The electrochemical oxidation of 4 μM GSH using various modified electrode surfaces at a scan rate of 0.4 V s^{-1} was investigated by cyclic voltammetry (CV) (Fig. 8). In the presence of 4 μM GSH, the bare ITO exhibits a small oxidation peak current (0.08 μA) during the anodic scan, which is caused by the oxidation of GSH. However, a dramatic change in the oxidation peak current (0.1 μA) is observed when the ITO electrode surface is modified with GO. The GO/ITO electrode shows a pair of quasi-reversible redox peaks,[44,45] due to the electrocatalytic activity of oxygen functional species on GO towards the GSH oxidation. Furthermore, the modified electrode enhanced the catalytic activity when laccase is immobilized on GO-modified ITO. However, the oxidation peak current (0.18 μA) is higher than the other electrodes when the modified electrode laccase/GO/ITO is tested in the same condition due to the effect of laccase.[39,40]

Electrochemical response toward GSH. The electrochemical sensing characteristics are studied by using cyclic voltammetry (CV) to estimate the quantitative detection of GSH. CV measurements of GSH at the modified electrode were carried

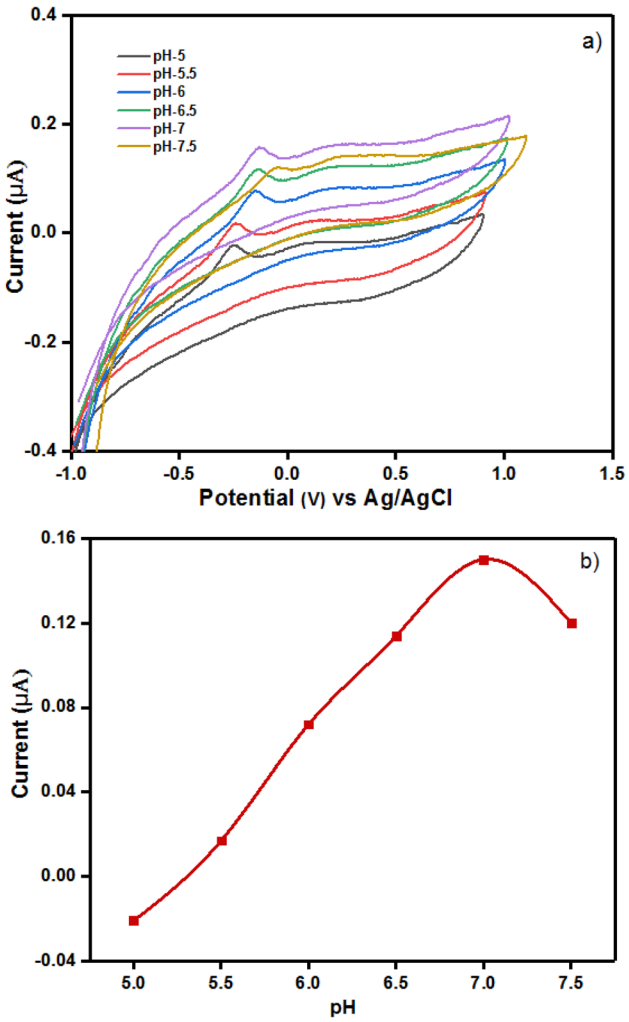

Fig. 7 (a) Cyclic voltammograms of 5 μM GSH at the surface of laccase/GO/ITO in PBS at pH values of 5, 5.5, 6, 6.5, 7, and 7.5 (b) plot of I_p *vs.* pH for the oxidation of GSH at the surface of laccase/GO/ITO.

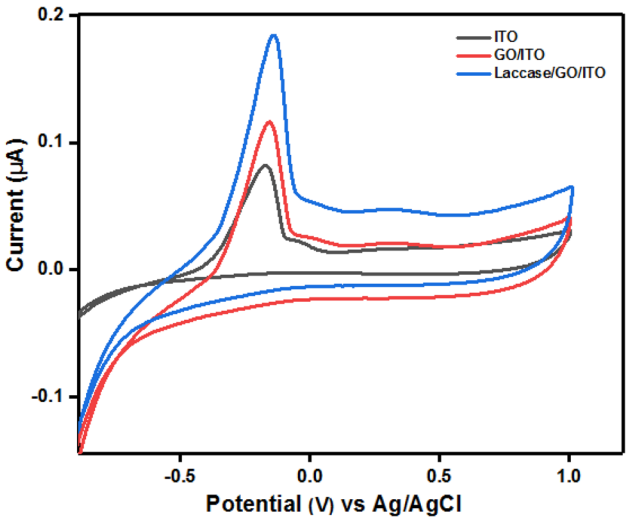

Fig. 8 Cyclic voltammograms of ITO, GO/ITO, and laccase/GO/ITO in PBS (pH = 7) containing 4 μM of GSH.

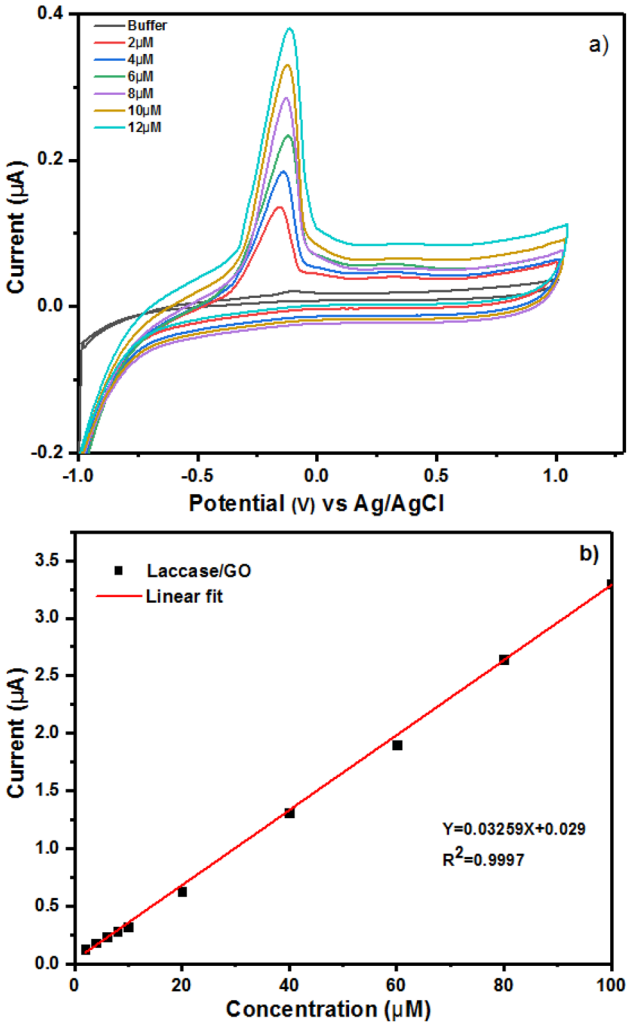

Fig. 9 (a) CV of laccase/Go/ITO in solutions containing different concentrations of GSH in PBS (pH = 7). (b) Linear curves of the anodic peak currents *vs.* GSH concentration.

out at the working electrode potential of 40 mV s^{-1} with various concentrations of GSH (Fig. 9a). The catalytic oxidation current increases as GSH concentration increases. The catalytic current obtained from the measurements is linear using 1 μM to 100 μM GSH, with a regression coefficient of $R^2 = 0.9997$, detection limit of 0.89 μM, limit of quantification of 2.70 μM, and high sensitivity (6.51 μA μM^{-1}) (Fig. 9b). These findings suggest that the modified electrode is suitable for the electrochemical determination of glutathione. Table 1 summarizes the comparison of detection limits utilizing laccase/GO/ITO electrode to other modified electrodes previously published in the literature.

Electrochemical impedance spectra (EIS) of analysis. One of the common electrochemical impedance spectra (EIS) is the Nyquist plot (Z_{im} *vs.* Z_{re}), which has a semicircular region on the Z_{re} axis that is observed at higher frequencies and is related to the electron-transfer-limited process, followed by a linear part at lower frequencies that represents the diffusion-limited electron transfer process. The diameter of the semicircle is equal to the surface electron-transfer resistance (R_{et}), which is managed by the electrode's surface modification.[28,57] Fig. 10 shows the EIS of the bare ITO, GO/ITO, laccase/GO/ITO modified electrode in 5 mM $[Fe(CN)_6]^{3-/4-}$ with frequency sweeping from 0.1 Hz to 1 MHz. According to the obtained spectra, it can be concluded that bare ITO demonstrates a response consistent with the electron-transfer-limited process, whereas R_{et} decreased with the incorporation of GO onto bare ITO. As a result, there was a conducting graphene oxide (GO) on the electrode surface, which indicates that the system is moving away from an electron-transfer-limited process and towards a diffusion-limited electron transfer process. However, the modified electrode (laccase/GO/ITO) exhibits almost a straight line (a) with a very small depressed semicircle due to the immobilization of enzymes on the surface of GO/ITO. This depressed semicircle shows the lower electron transfer resistance behaviour compared with the bare ITO electrode. The decrease in the value of electron transfer resistance (R_{et}) was caused by the immobilization of enzyme on the electrode surface.[30]

Selectivity, stability, and reproducibility. In order to determine the selectivity of the laccase/GO/ITO-based electrochemical biosensor, some possible interfering species, such as methionine, tryptophan, cysteine, and glucose, were investigated at identical experimental conditions. Cyclic voltammetry values were taken in 0.1 M PBS containing 100 μM methionine, 1 mM cysteine, 1 mM glucose, and 4 μM GSH individually (Fig. 11). It is clear that the main difference is the anodic peak as

Table 1 Comparison of different modified electrodes for electrochemical sensing of GSH

Sr. no.	Modified electrodes	Linear range	LOD	Ref.
1	GO/GCE	5–875 μM; 875 μM to 4.08 mM	5 μM	46
2	4-Amino-TEMPO/ERGO/GCE	1–254 μM	0.6 μM	47
3	AgNPs(TMSPED)–rGO/GC	0.1–2.75 μM	0.1 μM	48
4	GO/CdTe QDs	24–214.0 μM	8.3 μM	49
5	CuCoHCF/GO	5–90 μM	0.25 μM	50
6	NiHCF/AuNPs/CPE	0.1 μM to 1.4 mM	0.5 μM	51
7	Co–MOCP/CPE	2.5 μM–0.95 mM	2.5 μM	52
8	Cu–CoHCF/GCE	5–90 μM	2.5 μM	53
9	MWCNTs/SPE	5–20 μM	2 μM	54
10	NiONPs/GCE	12.5 μM to 2.3 mM	2 μM	55
11	Ni/ITO	5–840 μM	5 μM	56
12	Lacasse/GO/ITO	1–100 μM	0.89 μM	This work

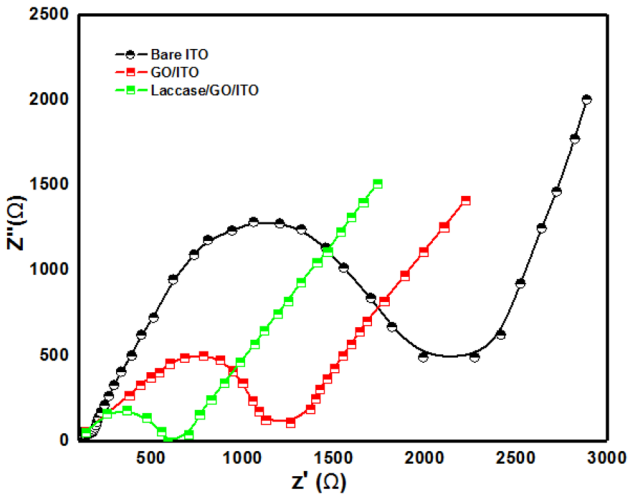

Fig. 10 Electrochemical impedance spectra (EIS) of bare ITO, GO/ITO and laccase/GO/ITO in 0.1 M KCl aqueous solution containing 5 mM $[Fe(CN)_6]^{3-/4-}$.

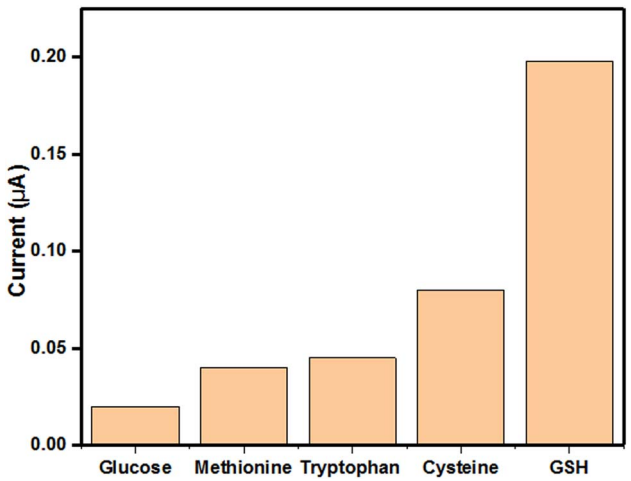

Fig. 11 Selectivity study of the laccase/GO/ITO base electrochemical biosensor.

the catalytic current of GSH oxidation reached a maximum at the applied potential. The presence of these electroactive species did not affect the selectivity on the measurement of GSH due to the low detection potential. These results suggest that the sensor electrode has excellent selectivity toward the detection of GSH.[47] The anti-interference capability of the laccase/GO/ITO electrode was evaluated by conducting CV measurements with 4 μM GSH in the presence of potential interferents, including 100 μM methionine, 1 mM cysteine, 1 mM tryptophan, and 1 mM glucose. Results revealed that the presence of other common interferences had no effect on the peak currents for the oxidation of GSH. These findings indicated that methionine, tryptophan, cysteine, glucose did not significantly interfere with GSH determination.[48]

Furthermore, the reproducibility of electrochemical sensors is a crucial aspect in deciding their practical application. As a result, we used seven different electrodes (a new one used each time) for the detection of 5 μM GSH under similar experimental conditions. Each individual sensor's electrochemical response was the average of 10 consecutive experiments. The result showed that a relative standard deviation RSD% of 3.2%. In addition, the repeatability was checked using five consecutive measurements on a single electrode. The results showed an RSD% of 2.7%. The long-term stability of the modified electrode was evaluated through repetitive CV scans over multiple cycles: the modified electrode was tested for a month in 5 μM GSH. The storage stability test demonstrated that the electrode retained over 95% of its initial response after 30 days of storage at 4 °C. The current response (μA) *vs.* time (days) showed minimal degradation for the modified electrode over 30 days, indicating good stability (Fig. 12). The above results show that the laccase/GO/ITO electrode has excellent stability and reproducibility.

Sensing mechanism of laccase/GO/ITO electrode. The working principles of the biosensor and its detection mechanism are shown in Fig. 13. The analyte is oxidized by the enzyme to oxidized glutathione (GSSG) and then regenerated through electrochemical reduction of GSSG. The resulting production of electrons at the working electrode are detected as current. Accordingly, the current is proportional to the concentration of the oxidized product and to the concentration of the analyte.[58,59]

Analysis of GSH in real samples. The analytical applicability of the sensor was further assessed by the determination of GSH in a real blood sample. Human whole blood was obtained from the health center of the university campus. Without further pretreatment, the solution was directly added to a stirring PBS solution at pH 7 (40.0 mL) into the voltammetric cell for analysis. The GSH concentration in the blood solution was found to be 20 μM. The recoveries were also estimated by adding GSH standards to the above solution. The results showed that the sensor gave acceptable recoveries between 95% and 105.1%. The results of actual sample analysis indicated that the proposed sensor could determine GSH in the blood sample.

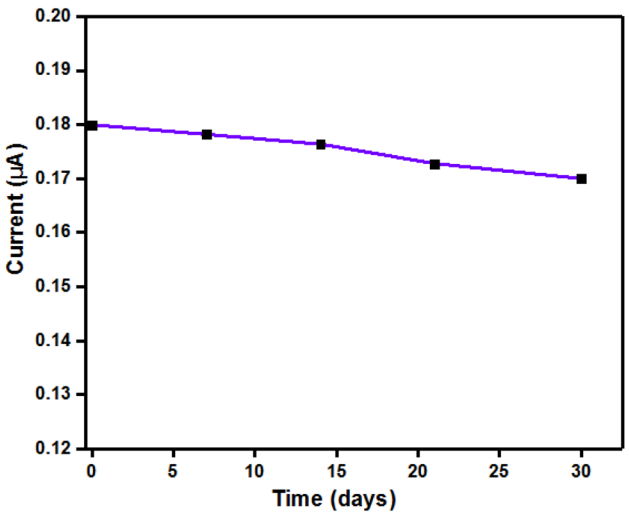

Fig. 12 Stability testing of the laccase/GO/ITO-based electrochemical biosensor.

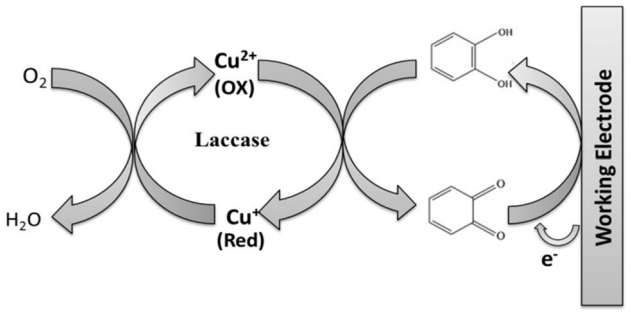

Fig. 13 Sensing mechanism of laccase-based electrochemical biosensor for the detection of GSH.

Conclusion

An electrochemical biosensor based on the immobilization of enzymes was developed for the detection of glutathione. The CV and EIS analyses performed on laccase/GO/ITO exhibited high electrocatalytic activity and the best selectivity toward GSH along with a linear dynamic range of 1 μM to 100 μM. In addition, the lower limit of detection was 0.89 μM and the limit of quantification was 2.70 μM with high sensitivity (6.51 μA μM^{-1}). The modified electrode has a high potential for the development of novel sensors due to its inexpensive cost of electrode material, simple fabrication method, and high sensitivity to GSH. The findings of this work suggest that GO could be employed as a promising sensing material along with enzyme for the detection of GSH. Also, this developed sensor can be successfully used to determine GSH in pharmaceutical and biological samples.

Data availability

The data sets generated during and/or analysed during the current study are available from the corresponding author on reasonable request.

Author contributions

Mrs Neeta Ukirade: conceptualization, investigation, methodology, explanation of results, writing of the manuscript. Mrs Upasana Choudhari: conceptualization, investigation, visualization, explanation of the results. Dr Sunil Bhapkar: conceptualization, investigation, visualization, format analysis. Dr Umesh Jadhav: conceptualization, investigation, visualization format analysis. Dr Shweta Jagtap: conceptualization, methodology, resources, visualization, supervision, reviewing and editing. Dr Sunit Rane: conceptualization, methodology, resources, visualization, supervision, reviewing and editing.

Conflicts of interest

There are no conflicts to declare.

Acknowledgements

One of the authors (Neeta Ukirade) is grateful to C-MET for providing the facility to carry out the research work for her PhD degree.

References

1 N. Varnakavi and N. Lee, *Sensors*, 2021, **21**(4), 1109.
2 R. Gaia, A. Spanu, S. Babudieri, G. Latte, G. Madeddu, G. Galleri, S. Nuvoli, P. Bagella, M. Demartis, V. Fiore, R. Manetti and P. Serra, *Sensors*, 2016, **16**(6), 780.
3 K. Nur Melis, S. Singh, G. Keles, S. Cinti, S. Kurbanoglu and D. Odaci, *Biosensors*, 2023, **13**(6), 622.
4 P. Mohankumar, J. Ajayan, T. Mohanraj and R. Yasodharan, *Measurement*, 2021, **167**, 108293.
5 A. Haleem, M. Javaid, R. Singh, R. Suman and S. Rab, *Sensors International*, 2021, 100100.
6 S. Malik, K. Muhammad and Y. Waheed, *Molecules*, 2023, **28**(18), 6624.
7 V. Singh, C. Singh, H. Ranjan and S. K. Pandey, *International Conference on Smart Grid and Energy (ICSGE)*, 2024, pp. 38–42.
8 V. Singh, C. P. Singh, H. Ranjan, G. Kumar, J. Jaiswal and S. Pandey, *Curr. Appl. Phys.*, 2024, **63**, 48–55.
9 C. Revathi, *Fundamentals and Sensing Applications of 2D Materials*, Woodhead Publishing, 2019, pp. 259–300.
10 N. Chauhan, K. Saxena, M. Tikadar and U. Jain, *Nanotechnol. Precis. Eng.*, 2021, 045003.
11 J. Yoon, M. Shin, T. Lee and J. W. Choi, *Materials*, 2020, **13**(2), 299.
12 U. Choudhari, S. Jagtap, N. Ramgir, A. K. Debnath and K. P. Muthe, *Rev. Chem. Eng.*, 2023, **39**(7), 1227–1268.
13 D. Holmannova, P. Borsky, T. Svadlakova, L. Borska and Z. Fiala, *Appl. Sci.*, 2022, **12**(15), 7865.
14 C. Cha, S. R. Shin, N. Annabi, M. R. Dokmeci and A. Khademhosseini, *ACS Nano*, 2013, **7**(4), 2891–2897.
15 T. Mathew, R. A. Sree, S. Aishwarya, K. Kounaina, A. G. Patil, P. Satapathy, S. Hudeda, S. More, K. Muthucheliyan, T. Kumar and A. Raghu, *FlatChem*, 2020, **23**, 100184.
16 D. Papageorgiou, I. Kinloch and R. Young, *Prog. Mater. Sci.*, 2017, **90**, 75–127.
17 U. Choudhari, N. Ramgir, D. Late, S. Jagtap, A. K. Debnath and K. P. Muthe, *Microchem. J.*, 2023, **190**, 108728.
18 S. Malik, J. Singh, R. Goyat, Y. Saharan, V. Chaudhry, A. Umar, A. A. Ibrahim, S. Akbar, S. Ameen and S. Baskoutas, *Heliyon*, 2023, 19929.
19 J. Zhang, J. Lei, Z. Liu, Z. Chu and W. Jin, *Environ. Res.*, 2022, **214**, 113858.
20 B. Kaur, R. Srivastava and B. Satpati, *RSC Adv.*, 2015, **5**(115), 95028–95037.
21 V. Singh, C. Singh, H. Ranjan, K. Harikrishnan and S. Pandey, *IEEE Trans. Electron Devices*, 2024, 5744–5753.
22 P. Lee, K. Ward, K. Tschulik, G. Chapman and R. Compton, *Electroanalysis*, 2014, **26**(2), 366–373.
23 H. J. Forman, H. Zhang and A. Rinna, *Mol. Aspects Med.*, 2009, **30**(1–2), 1–12.

24 N. Nesakumar, S. Berchmans and S. Alwarappan, *Sens. Actuators, B*, 2018, **264**, 448–466.
25 P. Baldrian, *Appl. Microbiol. Biotechnol.*, 2004, **63**, 560–563.
26 C. Wang, X. Sun, M. Su, Y. Wang and Y. Lv, *Analyst*, 2020, **145**(5), 1550–1562.
27 W. S. Hummers Jr and R. E. Offeman, *J. Am. Chem. Soc.*, 1958, **80**(6), 1339.
28 U. Anik, M. Çubukçu and F. Ertas, *Artif. Cells, Nanomed., Biotechnol.*, 2016, 971–977.
29 M. Bera, P. Gupta and P. K. Maji, *J. Nanosci. Nanotechnol.*, 2018, **18**(2), 902–912.
30 S. Malinowski, J. Jaroszyńska-Wolińska and P. Herbert, *J. Mater. Sci.*, 2019, **54**(15), 10746–10763.
31 Y. Shin, Y. Sa, S. Park, J. Lee, K. Shin, S. Joo and H. Ko, *Nanoscale*, 2014, **6**(16), 9734–9741.
32 Y. Li, S. Y. Yang and S. M. Chen, *Int. J. Electrochem. Sci.*, 2011, **6**(9), 3982–3996.
33 W. Zhou, W. Zhang and Y. Cai, *Sep. Purif. Technol.*, 2022, **294**, 121178.
34 G. Greczynski and L. Hultman, *Prog. Mater. Sci.*, 2020, **107**, 100591.
35 D. Krishna and J. Philip, *Applied Surface Science Advances*, 2022, **12**, 100332.
36 N. Hidayah, W. Liu, C. Lai, N. Noriman, C. Khe, U. Hashim and H. Lee, *AIP Conf. Proc.*, 2017, **1892**, 150002.
37 Y. Hongxia, Y. Yuxiang, H. Yan, Z. Yi and N. I. Chaoying, *J. East China Univ. Sci. Technol.*, 2019, **45**(6), 873–882.
38 S. Cheraghi, M. A. Taher, H. Karimi-Maleh, F. Karimi, M. Shabani-Nooshabadi and M. Alizadeh, *Chemosphere*, 2022, **287**, 132187.
39 B. Yuan, C. Xu, L. Liu, Q. Zhang, S. Ji, L. Pi, D. Zhang and Q. Huo, *Electrochim. Acta*, 2013, **104**, 78–83.
40 B. Liu, M. Wang and B. Xiao, *J. Electroanal. Chem.*, 2015, **757**, 198–202.
41 J. C. Fornaciari, L. C. Weng, S. M. Alia, C. Zhan, T. A. Pham, A. T. Bell, T. Ogitsu and N. Danilovic, *Electrochim. Acta*, 2022, **405**, 139810.
42 S. Alharthi, H. A. Batakoushy, S. A. Alharthy, M. O. Abd El-Magied and W. M. Salem, *Toxicol. Res.*, 2022, **11**(1), 245–254.
43 Y. Cai, Y. Zhang, S. Su, S. Li and Y. Ni, *Front. Biosci.*, 2007, **12**, 1946–1955.
44 J. Qu, Y. Wang, J. Guo, T. Lou and Y. Dong, *Anal. Lett.*, 2014, **47**(15), 2537–2547.
45 S. Lzaod and T. Dutta, *ACS Omega*, 2022, **51**, 47434–47448.
46 B. Yuan, X. Zeng, C. Xu, L. Liu, Y. Ma, D. Zhang and Y. Fan, *Sens. Actuators, B*, 2013, **184**, 15–20.
47 B. Yuan, C. Xu, D. Zhang, R. Zhang, H. Su, P. Guan, J. Nie and C. Fernandez, *Electrochem. Commun.*, 2017, **81**, 18–23.
48 V. Vinoth, J. Wu, A. Asiri and S. Anandan, *Ultrason. Sonochem.*, 2017, **39**, 363–373.
49 Y. Wang, J. Lu, L. Tang, H. Chang and J. Li, *Anal. Chem.*, 2009, **81**(23), 9710–9715.
50 V. V. Sharma, L. Guadagnini, M. Giorgetti and D. Tonelli, *Sens. Actuators, B*, 2016, **228**, 16–24.
51 P. C. Pandey and A. K. Pandey, *Analyst*, 2012, **137**(14), 3306–3313.
52 B. Yuan, R. Zhang, X. Jiao, J. Li, H. Shi and D. Zhang, *Electrochem. Commun.*, 2014, **40**, 92–95.
53 V. V. Sharma, L. Guadagnini, M. Giorgetti and D. Tonelli, *Sens. Actuators, B*, 2016, **228**, 16–24.
54 P. T. Lee and R. G. Compton, *Sens. Actuators, B*, 2015, **209**, 983–988.
55 B. Yuan, X. Zeng, D. Deng, C. Xu, L. Liu, J. Zhang, Y. Gao and H. Pang, *Anal. Methods*, 2013, **5**(7), 1779–1783.
56 H. Tian, T. Wang, Y. Fu, Y. Yu, C. Guo and J. Hu, *J. Electrochem. Soc.*, 2014, **161**(9), 191.
57 U. Choudhari and S. Jagtap, *AIP Adv.*, 2021, **11**(12), 125327.
58 J. Chen, Z. He, H. Liu and C. Cha, *J. Electroanal. Chem.*, 2006, **588**(2), 324–330.
59 N. Ukirade, S. Jagtap and S. Rane, *Hybrid Advances*, 2023, **3**, 100042.